Multi-variable Optimization to Improve Temperature Uniformity in Burn-in Applications Subjected to Significant Thermal Shadowing

by

AJINKYA SUHAS MAHAJAN

Presented to the Faculty of the Graduate School of

The University of Texas at Arlington in Partial Fulfillment

of the Requirements

for the Degree of

MASTER OF SCIENCE IN MECHANICAL ENGINEERING

THE UNIVERSITY OF TEXAS AT ARLINGTON

August 2019

Acknowledgments

My sincere gratitude goes to Dr.Dereje Agonafer, for giving me the opportunity to work in his EMNSPC Research lab on my thesis research. He has been a constant guiding light and a source of motivation for me and all other members of the lab.

I am thankful to Dr.Haji A. Sheikh and Dr.Andrey Beyle for being a part of my thesis defense committee. A special thanks go to Derek Biggs and Jason Cullen from Plastronics Inc. for being present for the thesis defense. I really appreciate their constant guidance and support during my Internship at Plastronics Inc.

I am very much grateful to Abel Misrak for the guidance he provided amidst his doctorate research. I would like to thank all my friends who always been there to support just like family. I thank my roommates and lab mates Satyam, Pratik and Pardeep for their constant moral support throughout my master's degree and especially during this research. Finally, I would like to thank my family for providing with the opportunity to study and pursue my Masters in the United States. Without their support, this journey would not have completed.

August 1st, 2018

Abstract

MULTI-VARIABLE OPTIMIZATION TO IMPROVE TEMPERATURE UNIFORMITY
IN BURN-IN APPLICATIONS SUBJECTED
TO SIGNIFICANT THERMAL SHADOWING

Ajinkya Suhas Mahajan, MS

The University of Texas at Arlington, 2019

Supervising Professor: Dereje Agonafer

Burn-in test typically employs voltage and/or temperature to accelerate the appearance of latent reliability defects in semiconductor devices. As a result, burn-in becomes a critical step in the parts screening process and is the primary technique to eliminate defective parts in the early phase of the product life. Thermal control in burn-in processes is generally achieved by either active or passive thermal controlling. In an active thermal control, each device has an individual temperature monitoring system to maintain a specific temperature in which the cooling/heating of each socket is controlled by an individual fan or heater. Whereas in passive thermal control, a single fan provides convective heat transfer to an array of devices. Recent research regarding burn-in process suggests that passively controlled sockets are impacted more by temperature and airflow variation in burn-in ovens when compared to actively controlled sockets.

In our study, a fan and two sockets were placed linearly and the airflow characteristics were examined past the first-row socket. An air deflector was designed on the ceiling of the oven between the two sockets and was optimized for its location, size, and orientation to improve the heat transfer characteristic of the second-row socket.For analysis and optimization, socket and burn-in chamber design specification were

obtained from Plastronics Inc. 3D CAD model was designed in Solidworks and was solved numerically considering appropriate boundary conditions in Solidworks native Flow Simulation. Finally, Multi-variable design optimization and response surface methodology were performed to propose an optimum design for air deflector to increase the thermal performance of socket in the burn-n application.

Table of Contents

List of Illustrations

List of Tables

Chapter 1

Introduction

1.1Burn-inprocess

Understanding the bathtub curve is essential to study the Burn-in process. It is also called a shape of the failure rate over time for most products. In a batch of products (semiconductor devices), if one is going to fail, it will most likely fail soon after putting into use, in its early failure period. In figure 1-1 units that make it through its early failure period (Stage 1) are more likely to last through their expected lifetime until they start failing because they wear out (Stage 3). So we use burn-in to get units through early failure period, rather than after they reach to customers.

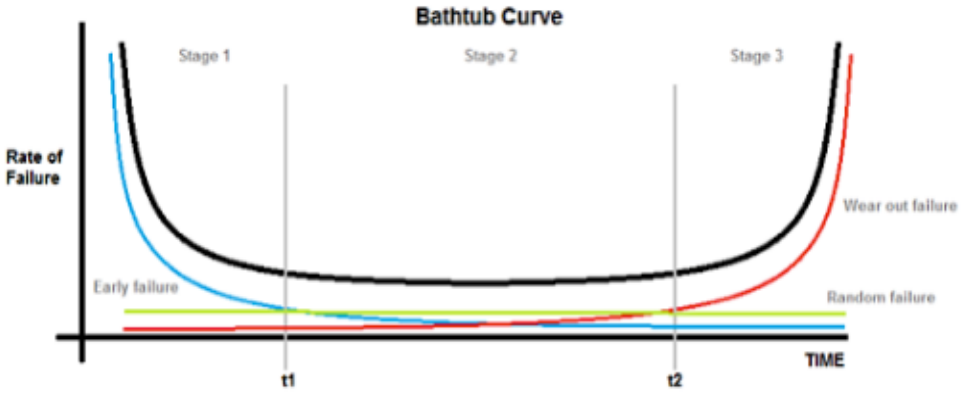

Figure 1-1 Bathtub Curve [1]

The burn-in process condenses the normal early failure period from weeks or month down to a few days. Cycling the power ON and OFF accelerates any failure that will happen due in rush current and thermal expansion. Keeping the burn-in chamber at a higher temperature further accelerates early failure. Mostly, the case temperature of the device is raised to 125°C-130°C and keep stable at 10 minutes in the Burn-in chamber.

The rule of thumb is that the failure rate will double at every 10°C. So running the burn-in chamber at 55°C to 60°C we can expect the products to fail much faster than at room temperature. The failures can be classified as a dielectric, conductor, metallization, electro migration, mouse-bites failures etc. which are mostly dormant and appears randomly in semiconductor device life cycle. The units that fail burn-in are rejected and never reach the customer. Burn-in can find a single bad part – if one unit fails or an entire batch of parts if many units start to fail for the same reason. When that happens, engineers investigate to discover the root cause and work with component suppliers to resolve the issue. So in summary; we use burn-in to weed out early failure due to defects in Stage 1 of the Bathtub curve to stabilize some components and to help us get long term reliability for semiconductor devices.

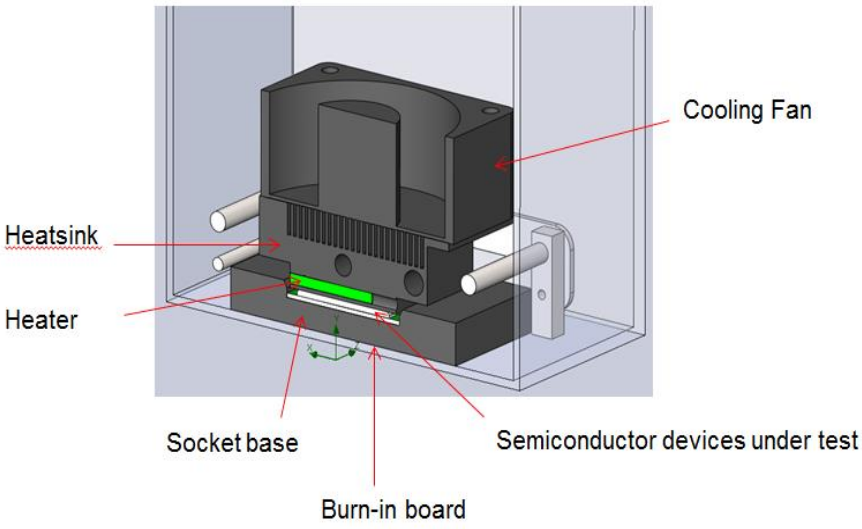

Figure 1-2 Burn-in socket layout

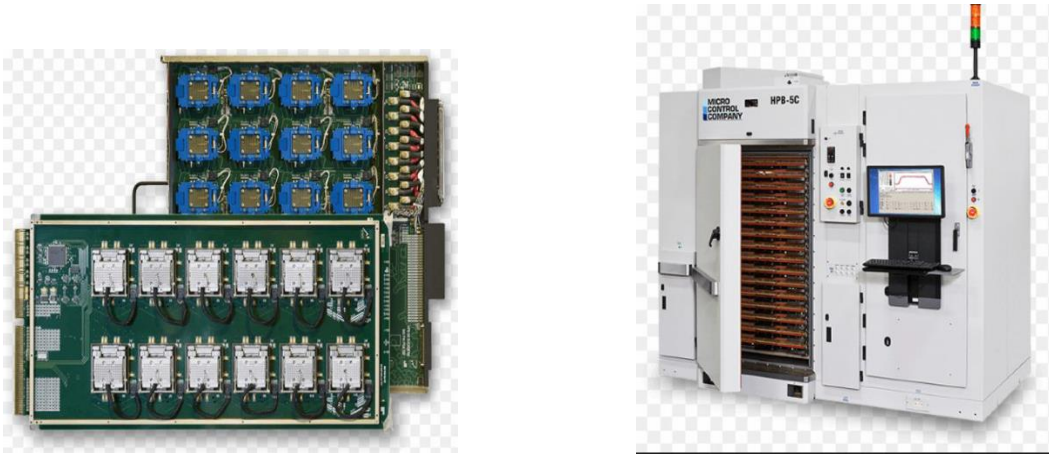

Figure 1-3 Burn-in boards (left) and Burn-in chamber (right) [3]

1.2 Burn-in Sockets

In the Burn-in process, two kinds of sockets are used widely, namely Passive Thermally Controlled sockets shown in figure 1-4 and Active Thermally Controlled Sockets in figure 1-5. In passive thermal controlled sockets, cross-flow of air is provided over the arrays of sockets for cooling whereas heat is extensively generated only by semiconductor devices. Therefore, It takes a little while for passive thermal controlled sockets to attain the target case temperature of 125°C than that of active thermal controlled sockets.

There are no other auxiliary devices like a top fan or additional heater provided to heat up, and cooling is provided to the socket in Passive thermally controlled sockets. The main reason to use Passive thermally controlled socket over Active thermal controlled socket is the cost. Some small/ inexpensive devices are used in Passive thermally controlled sockets.

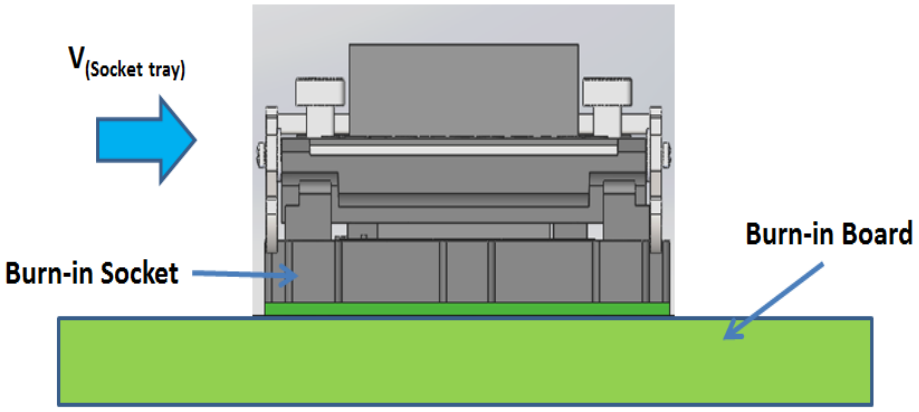

Figure 1-4 Passive Thermal Controlled Sockets

On another hand, Active thermal controlled sockets are those in which each socket is provided with individual temperature monitoring to maintain a specific temperature of the case. In Active thermally controlled sockets, cooling/heating of each socket is controlled by individual fans or heaters for each socket. These sockets are widely used for large and expensive semiconductor devices to test. In some chambers, the top air valve is also provided where a fan cannot be mounted over sockets. The main advantage of Active thermal controlled sockets is there is temperature uniformity across sockets, which cannot be observed in the case of passive thermal controlled sockets.

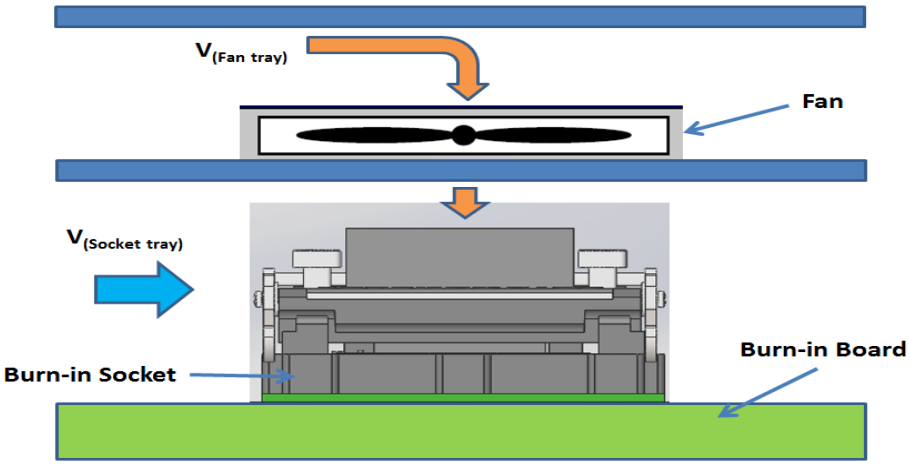

Figure 1-5 Active Thermal Controlled Sockets

1.3 Motivation

In passive thermally controlled sockets as air travels through the oven its temperature increases (ambient temperature) as shown in figure 1-6 due to obtaining heat while traveling through consecutive sockets. As a result, the case temperature of semiconductor devices in socket 2 will be at a higher temperature than that of case temperature in socket 1. Besides, there will be thermal shadowing effect of socket 1 on socket 2, which will further worsen the case temperature difference between two sockets.

The main purpose of this study is to design an air diverter over the ceiling of the test chamber by using CAD, which will reduce thermal shadowing effect observed. Also, Multi-Variable Optimization and Surface Response Methodology are incorporated to evaluate the optimum position of the diverter, which will reduce the case temperature difference between two sockets

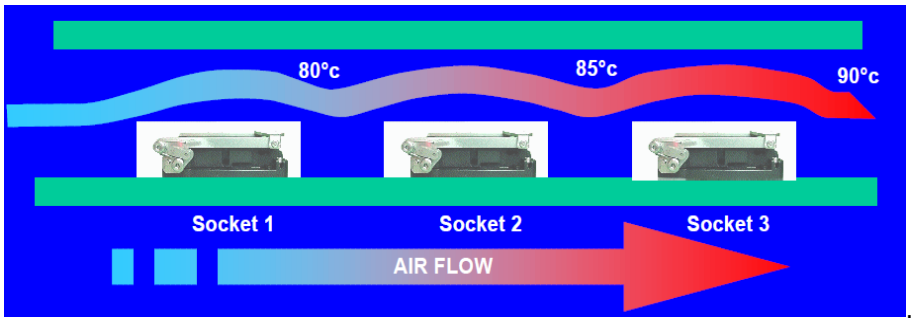

Figure 1-6 Conventional System (Passive Thermal Control) [2]

Chapter-2

Model Setup

2.1 Ideal Burn-in chamber setup for passive thermal controlled sockets:

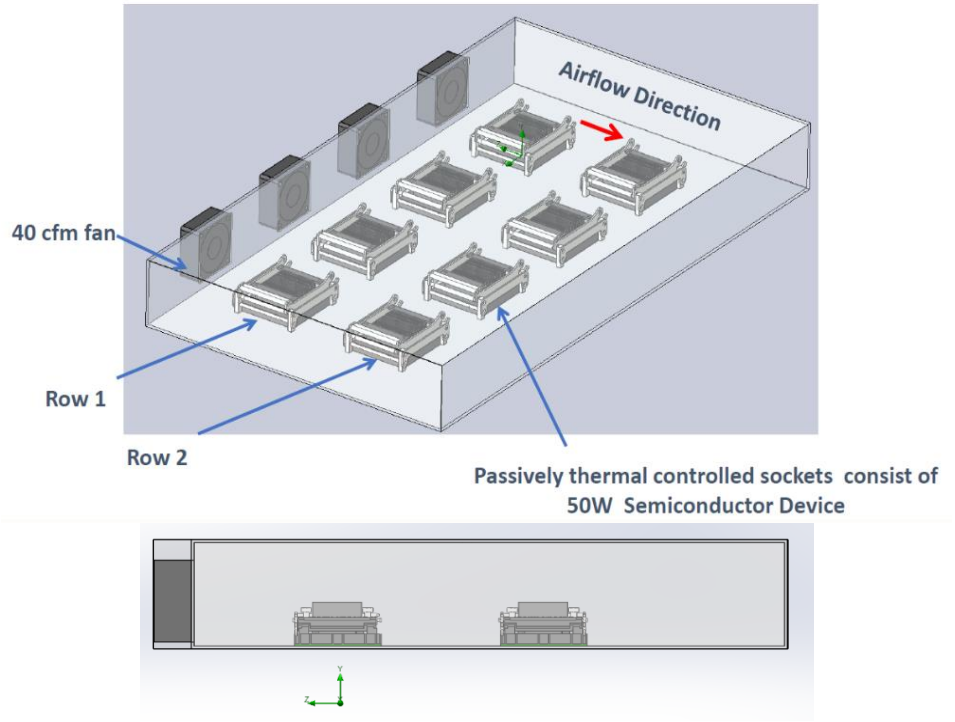

Figure 2-1 Ideal Burn-in Chamber

Figure 2-1 shows the ideal burn-in chamber model in Computational Fluid Dynamics where 40cfm fans are at inlet and outlet is having environmental pressure conditions of 1 atmosphere. Design specifications of Burn-in sockets were obtained from Plastronics Inc., and by using Computer-Aided Designing sockets are designed in SolidWorks. The sockets are arranged in Row 1 and Row2 as shown in figure 2-1 on 12 layers Non-isotropic PCB material. Ultem 2210, an enhanced flow Polyetherimide filled

with 20% Glass fiber is used in socket body. The Silicon semiconductor device placed in the nest of the socket produces 50W of power. Copper rods as shown in figure 2-2 are used to make electrical contact to the semiconductor device. A significant amount of heat is dissipated toward heatsink, and very less amount is dissipated to PCB board through copper connectors [6,7]. Appropriate thermal interface material is applied between heatsink and case of the semiconductor devices.

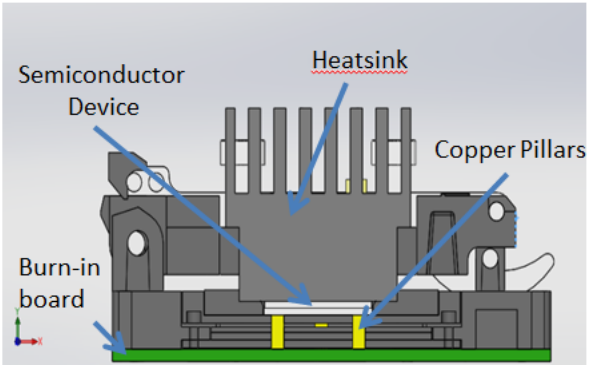

Figure 2-2 Cross-section of Passive Thermal Controlled Socket

Fans used in the simulation studies are 40 cfm External Inlet fans. The data required for creating fan curves were obtained from Plantronics Inc., and fan performance curve shown in fig below was generated to emulate physical fans used in the simulation. The inlet is assigned with the above generated External inlet fans as soon in figure 2-3 .

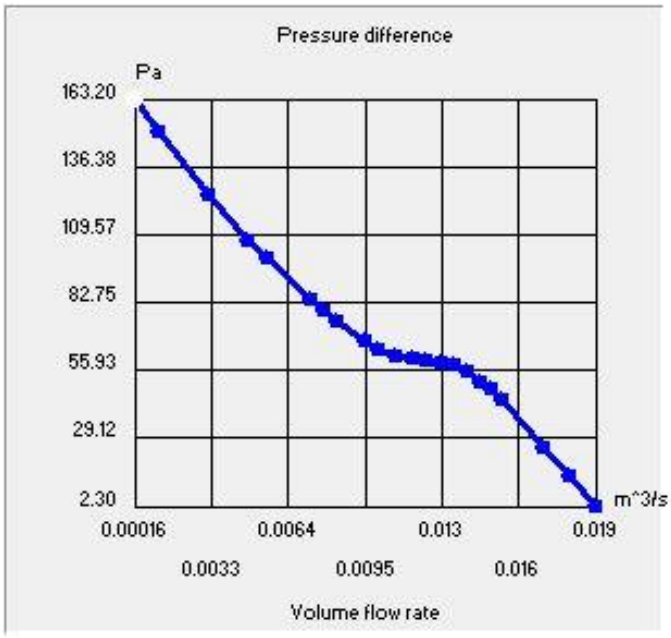

Figure 2-3 Fan Curve

Symmetric boundary conditions can be a huge advantage to reduce the flow problem , which can further reduce the time required to solve the analysis [5,8]. Therefore to improve the efficiency of the Simulation study, the symmetric computational domain is selected in x transitional axis as shown in figure 2-4. In this way, the effect of the flow field of other fans in the model setup can be considered.

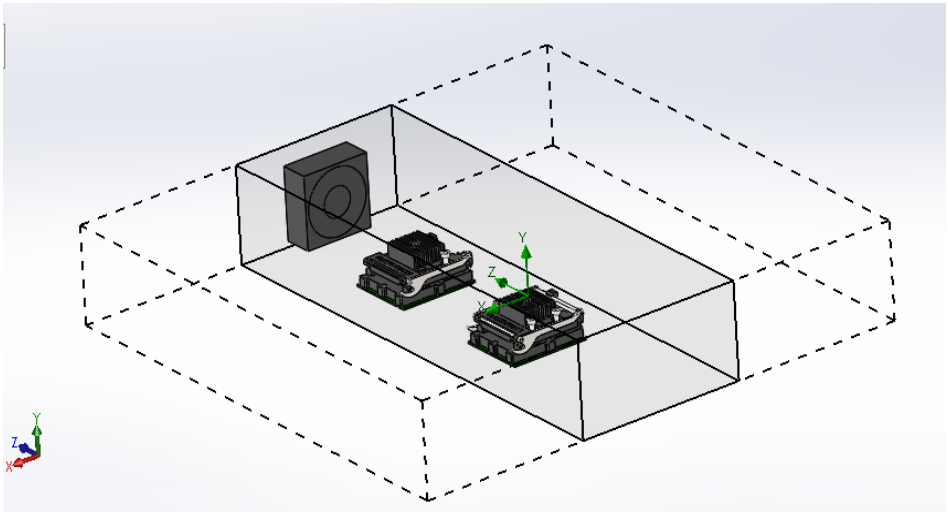

Figure 2-4 Symmetric boundary conditions for the burn-in process

2.2 Burn-in chamber with Air Deflector

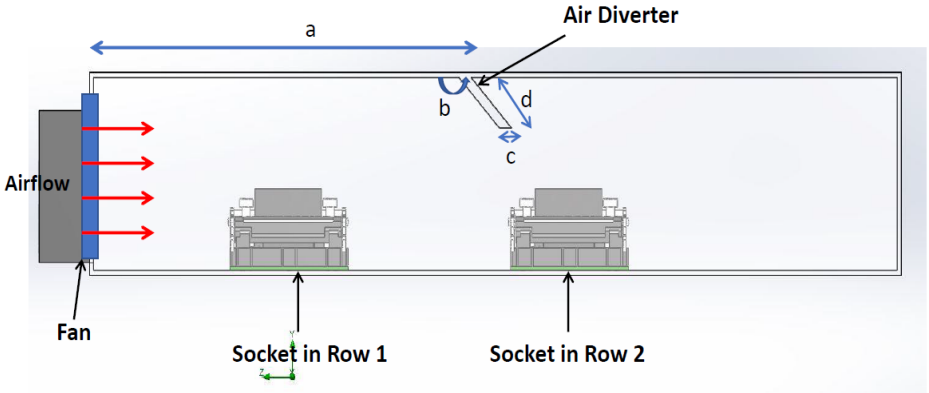

Figure 2-5 Burn-in chamber with deflector at intuitive position

For comparative studies , another model of the burn-in process was designed using Air diverter at the intuitive position shown in figure 2-5. The air diverter was designed between Socket 1 and Socket 2 to reduce the effect of thermal shadowing

occurring in Passive thermal controlled sockets.[5] The distance at which the diverter was placed from the fan “a” is 180mm, the angle the diverter makes with the ceiling of the chamber “b” is 135°, the width of the diverter “c” is 6mm, and the height “d” of 28 mm was choosen initially.

Chapter-3

Computational Fluid Dynamics for Baseline Studies

In this study internal flow analysis type in SolidWorks Flow Simulation a CFD package is used. Internal flow analysis generally used when the flow is bounded by other solid surfaces like socket and burn-in chamber in our case. Generally the burn-in process is carried out for 10 minutes therefore this study is time dependent on the analysis time of 600 sec. The fluid consider is Air at an ambient temperature of 25°C which is inlet through. Each of the sockets is having a semiconductor electronic device which is used for burn-in creates 50 W each. Average surface temperature goals are created on the case of each semiconductor devices to monitor there temperature for convergence.

3.1 Meshing and boundary treatment:

Traditional CFD systems generally used Body-fitted algorithms. As shown in figure 3-1(a) ,Unstructured meshes are mostly used for complicated geometries by creating irregularly distributed notes around the geometry. On the other hand, for simpler geometries, structured meshes are used as shown in figure 3-1(b). Combination of structured and unstructured meshes figure 3-1(c) can also be used where the unstructured mesh is created near the wall . The nodes generation for these body-fitted meshes starts from the solid surfaces; therefore, these meshes are highly dependent on the CAD geometry. Mesh generation usually fails if there is any defect on the surface of the geometry. To solve these issue, users have to refine the surface by creating numerous nodes in the CAD geometry area, which are usually insignificant from CFD point of view.

In this study, Immersed-body mesh figure 3-1(d) is used. The creation of nodes for this mesh starts independently from the geometry. Immersed body mesh can intersect

the boundary between solids and fluids, which makes it easy to use cartesian- based mesh which is generally set of cuboids(rectangular cells) formed by dividing the rectangular computational domain. Taking this advantage in Immersed-body mesh, adaptive mesh refinement becomes possible. Figure 3-1 shows the mesh cut plot of the burn in chamber with air diverter , after applying adaptive mesh refinement.[4]

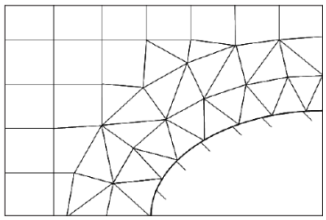

Figure 3-1 a

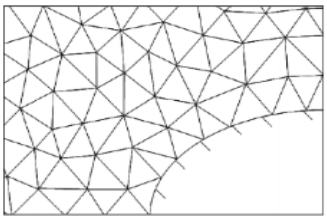

Figure 3-1 b

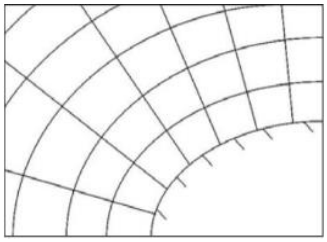

Figure 3-1 c

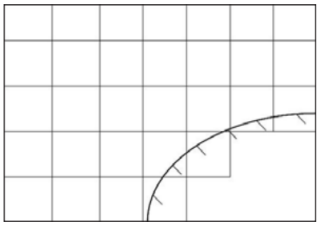

Figure 3-1 d

Figure 3-1 Types of Mesh structure [4]

A local initial meshing with fine mesh setting is used between the inter-fin spacing of the heatsink to capture the flow accurately and to perform channel refinement. This is achieved by adding a solid material that occupies this spacing and by assigning local initial mesh to that volume. After applying refinement settings, the body is excluded from the analysis with the help of component controls options.

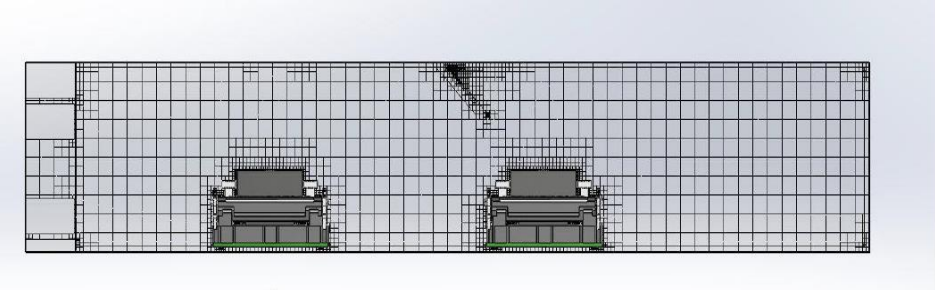

Figure 3-2 Adaptive mesh refinement cut plot

3.2 Mathematical Modelling:

By using Cartesian-based mesh [4] conjugate multi-physics problem can be solved, i.e. fluid flow analysis in the fluid region and heat transfer calculations in solid region. By using Navier-Stokes equations which is the formulation of mass, momentum, and energy conservation laws, fluid flow region is solved. SolidWorks Flow Simulations uses the Lam-Bremhorst modified k-epsilon model to solve its turbulence model.

$$\frac{\partial \rho}{\partial t} + \frac{\partial \rho u_i}{\partial x_i} = 0 \qquad 1$$

$$\frac{\partial \rho u_i}{\partial t} + \frac{\partial}{\partial x_j}\left(\rho u_i u_j\right) + \frac{\partial P}{\partial x_i} = \frac{\partial}{\partial x_j}\left(\tau_{ij}\tau_{ij}^R\right) + S_i \qquad 2$$

$$\frac{\partial \rho H}{\partial t} + \frac{\partial \rho u_i H}{\partial x_i} = \frac{\partial}{\partial x_j}\left(u_j\left(\tau_{ij}\tau_{ij}^R\right) + q_i + \frac{\partial \rho}{\partial t} - \tau_{ij}^R \frac{\partial u_i}{\partial x_i} + \rho\varepsilon + S_i u_i + Q_H\right) \qquad 3$$

$H = h + \frac{u^2}{2}$

The heat conduction in solids is solved by following equation (4)

$$\frac{\partial pe}{\partial t} = \frac{\partial}{\partial x_i}\left(\lambda_i \frac{\partial T}{\partial x_i}\right) + Q_H \qquad 4$$

3.3 Results with and without air deflector:

In figure 3-3 the average target temperature of Row 2 socket without using Air Diverter was noted to be 204°C after 10 minutes. By introducing air diverter at an intuitive position over the ceiling of the burn-in chamber, the average target temperature of Row 2 socket was reduced to 160°C, 21.56% reduction is observed in figure 3-4.

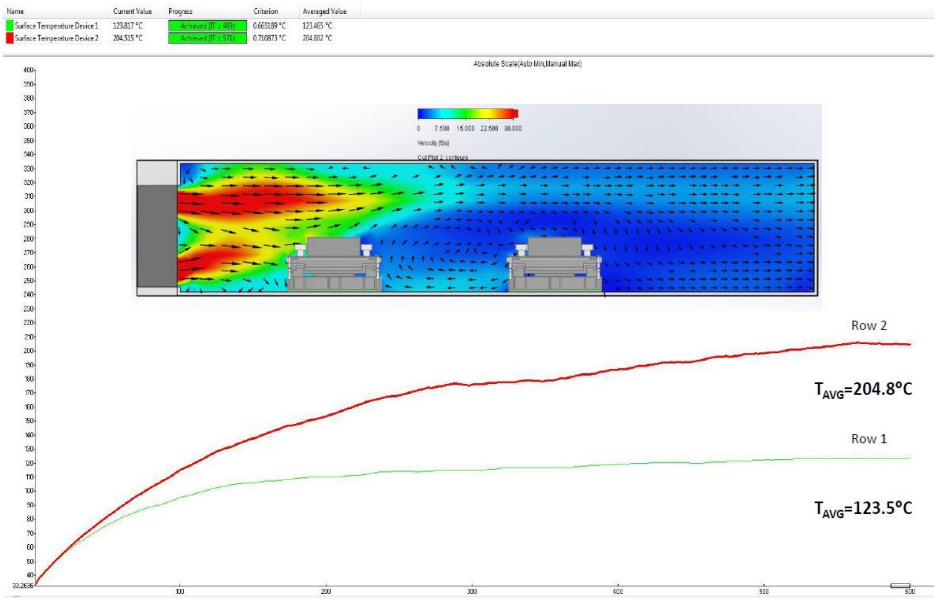

Figure 3-3 Results and Temperature Cut-plot without Air deflector

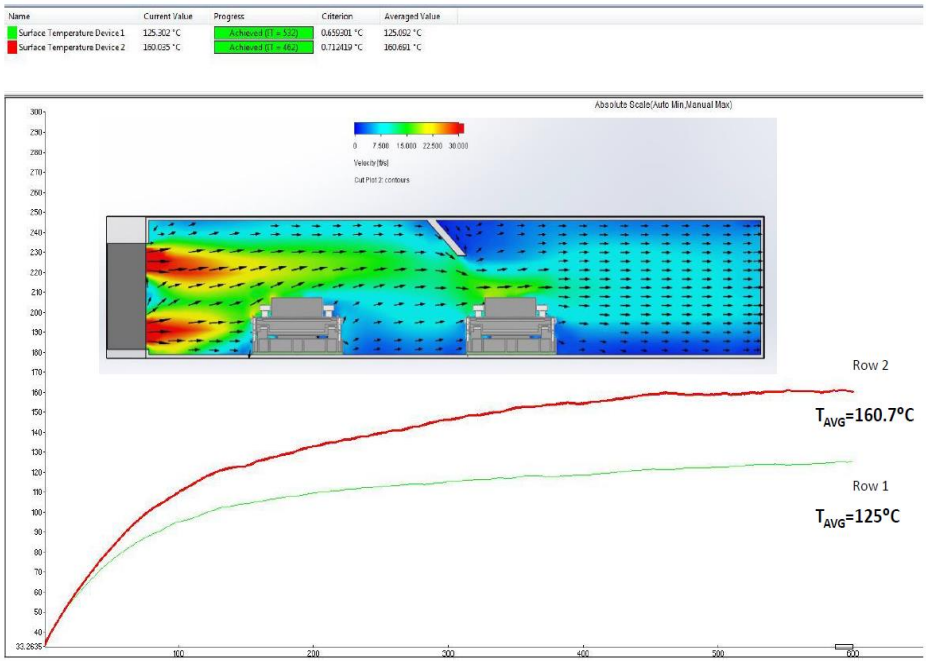

Figure 3-4 Results and Temperature Cut-plot without Air deflector

.

Chapter-4

Multi-variable Optimization Methodology

4.1 Variables of Air Deflector for Optimization:

Input variables are selected as soon in the figure 4-1 where a is the distance of diverter from the fan, 'b' is an angle deflector is making with the ceiling of the burn-in chamber, c is the width and d is the height of an air deflector. The input variables are allowed to vary between the values specified in the table while calculating the optimal solution. The average surface temperature goal for convergence is selected as T_1 for case temperature of the socket in Row 1 and T2 for case temperature of the socket in Row 2. The objective function to minimize in our study is assigned by goal ($T_2 - T_1$).

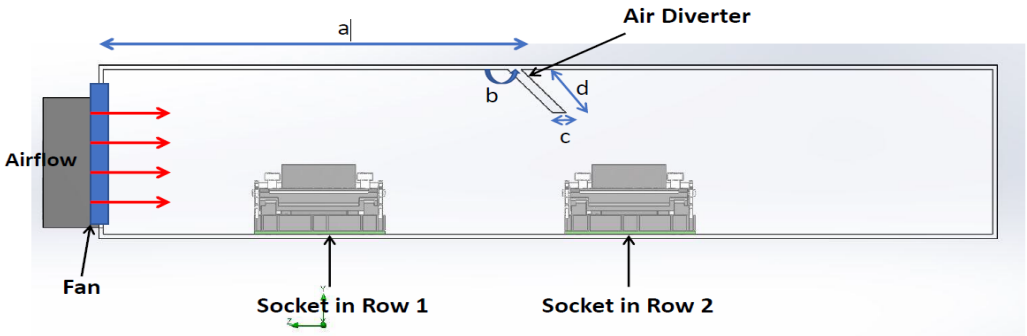

Figure 4-1 Input variables for Air deflector

4.2 Design of Experiments for Optimization

Design of Experiments(DoE) is the procedure of planning and finding the interaction between the input variables and output variables to get the predetermined results. Previous researcher implemented CVSAM for obtaining effective thermal conductivity and its sensitivity.[9-14] These calculated sensitivity can be advantageous in determining

the reliability of the system. Similar methods may be useful in calculating sensitivities. However, DOE performs better in terms of optimization of multivariable components, where one need not calculate sensitivity. Multi parameters tool uses various sampling method to derive these Design of Experiments as per user input. We have created 45 Experiments in DoE. The accuracy of the optimized solution is directly proportional to the number of experiments we are going to create. This is the reason the number of experiments is high for this study as shown in figure 4-2. Each experiment is solved by using a CFD package SolidWorks Flow Simulation to plot the Surface Response for finding the optimal design point for experiments.

	Distance from fan (a)	Length of deflector	Angle with ceiling[°]	Width of Deflector [mm]	T1 Surface Temperature Device 1	Surface Temperature Device 2 [°C]	T2
Experiment 1	170.6818182	17.86363636	84.54545455	35.45454545	123.6906558	173.7320242	50.04136846
Experiment 2	178.8636364	16.90909091	22.72727273	18.27272727	124.5856801	170.0428526	45.45717251
Experiment 3	152.2727273	35.04545455	66.36363636	36.68181818	124.4087275	158.1862364	33.77750896
Experiment 4	168.6363636	35.52272727	28.18181818	15.81818182	127.3286371	134.403105	7.074467894
Experiment 5	164.5454545	20.72727273	26.36363636	57.54545455	123.7874537	164.2094932	40.42203947
Experiment 6	221.8181818	32.65909091	31.81818182	17.04545455	125.9723606	157.3373658	31.36500524
Experiment 7	225.9090909	25.97727273	24.54545455	37.90909091	125.9326058	174.1357278	48.20312207
Experiment 8	142.0454545	18.81818182	51.81818182	44.04545455	122.927863	179.7170763	56.78921324
Experiment 9	160.4545455	28.36363636	82.72727273	51.40909091	123.5019283	159.386179	35.88425069
Experiment 10	180.9090909	26.45454545	40.90909091	39.13636364	124.6934611	151.1715598	26.47809867
Experiment 11	158.4090909	15	57.27272727	20.72727273	124.5395186	184.9002156	60.36069703
Experiment 12	203.4090909	18.34090909	50	7.227272727	124.7528875	163.3835053	38.63061776
Experiment 13	172.7272727	26.93181818	11.81818182	19.5	124.1257589	169.8166849	45.69092604
Experiment 14	230	24.06818182	62.72727273	47.72727273	124.3069823	153.9388768	29.6318945
Experiment 15	166.5909091	19.77272727	68.18181818	58.77272727	124.4121273	170.3743108	45.96218346
Experiment 16	154.3181818	31.70454545	64.54545455	10.90909091	124.3870252	160.7541688	36.36714364
Experiment 17	199.3181818	25.5	86.36363636	41.59090909	124.4089873	152.2276302	27.81864284
Experiment 18	209.5454545	31.22727273	71.81818182	8.454545455	126.2538161	135.1013775	8.847561438
Experiment 19	150.2272727	22.63636364	39.09090909	12.13636364	124.4557797	168.9638909	44.50811119
Experiment 20	193.1818182	34.56818182	77.27272727	48.95454545	126.6398001	139.7085997	13.0687996
Experiment 21	148.1818182	20.25	19.09090909	34.22727273	123.8989521	166.1512989	42.2523468
Experiment 22	187.0454545	27.88636364	42.72727273	6	125.4944102	143.0824037	17.58799346
Experiment 23	189.0909091	34.09090909	55.45454545	25.63636364	126.6865152	135.8167504	9.13023518
Experiment 24	223.8636364	32.18181818	79.09090909	31.77272727	126.5683638	136.5561065	9.987742719
Experiment 25	176.8181818	30.75	90	23.18181818	124.384515	155.3290273	30.94451226
Experiment 26	227.9545455	24.54545455	53.63636364	21.95454545	123.7200256	153.6139643	29.89393876
Experiment 27	205.4545455	17.38636364	75.45454545	52.63636364	124.1028519	168.9457488	44.84289688
Experiment 28	201.3636364	29.31818182	20.90909091	56.31818182	125.561901	162.6586986	37.09679762
Experiment 29	146.1363636	28.84090909	48.18181818	53.86363636	123.2023272	156.7532657	33.5509385
Experiment 30	217.7272727	16.43181818	30	29.31818182	124.1535149	171.7402398	47.58672488
Experiment 31	162.5	21.68181818	80.90909091	9.681818182	123.2599125	173.3440406	50.08412813
Experiment 32	174.7727273	36	37.27272727	50.18181818	126.851624	134.3512693	7.499645215
Experiment 33	207.5	22.15909091	88.18181818	14.59090909	124.5247815	154.3325921	29.80781055
Experiment 34	156.3636364	29.79545455	13.63636364	46.5	124.6462679	158.6256158	33.97934794
Experiment 35	211.5909091	23.59090909	17.27272727	13.36363636	124.0305149	179.3561297	55.32561482
Experiment 36	191.1363636	21.20454545	10	40.36363636	124.4651999	181.7685829	57.30338299
Experiment 37	185	23.11363636	60.90909091	24.40909091	123.9879625	156.2920489	32.30408641
Experiment 38	195.2272727	27.40909091	59.09090909	60	124.7112201	148.5693921	23.85817207
Experiment 39	140	30.27272727	35.45454545	26.86363636	124.3707047	154.6966289	30.32592418
Experiment 40	197.2727273	33.13636364	15.45454545	33	125.4090825	172.2974721	46.88838959
Experiment 41	215.6818182	15.95454545	70	28.09090909	124.3953381	170.4431986	46.0478605
Experiment 42	144.0909091	25.02272727	73.63636364	30.54545455	122.6301729	173.2836352	50.65346233
Experiment 43	219.7727273	33.61363636	46.36363636	45.27272727	126.0503318	140.8810425	14.83071068
Experiment 44	182.9545455	15.47727273	44.54545455	42.81818182	124.3971867	174.3769878	49.97980111
Experiment 45	213.6363636	19.29545455	33.63636364	55.09090909	124.8786165	166.8002282	41.92161172

Figure 4-2 Design of Experiments

Notification	Description	Variable Range
a	The position of deflector from fan	140mm<**a**<230mm
b	Angle with ceiling	10°<**b**<90°
c	Width of deflector	6mm<**c**<60mm
d	Length of deflector	15mm<**d**<36mm

Table 4-1 Input variables with a range

4.3 Multi-variable Response Surface-based optimization:

With the help of the design of experiments, we obtained a response surface as shown in Figure 4-3. With the help of this plots, we can study how the case temperature difference between two sockets (T_2-T_1) varied against the position of deflector from the fan, the width, height and angle the deflector is making with the ceiling. The optimum position of deflector will be calculated by minimizing the objective function (T_2-T_1). An optimal point corresponding to a minimum of the output parameter will be added to our Design of Experiments. Five such optimal points were calculated on the response surface, and the minimum of them was selected. The minimum of objective function occurs when the position of deflector from the fan, the angle with the ceiling, the width and length of the deflector is 191.37mm, 46.6°,6mm, and 36mm respectively.

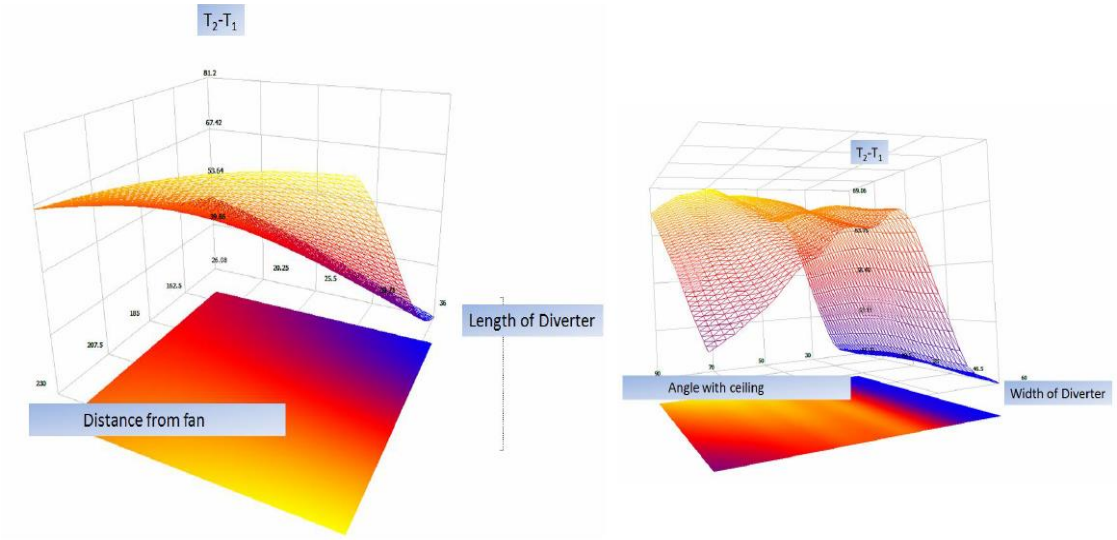

Figure 4-3 Response Surface

Chapter-5

Results and Future Work

5.1 Results

Optimal position and orientation of air diverter were achieved by using Multi-Variable design optimization to reduce thermal shadowing in the burn-in application. As shown in figure 5-1 the difference between average case temperature of both the devices was mere 6.4°C after utilizing the optimal design point obtained from the response surface. The average case temperature difference between two sockets was reduced to 92.12% from the one without having deflector at an optimized position.

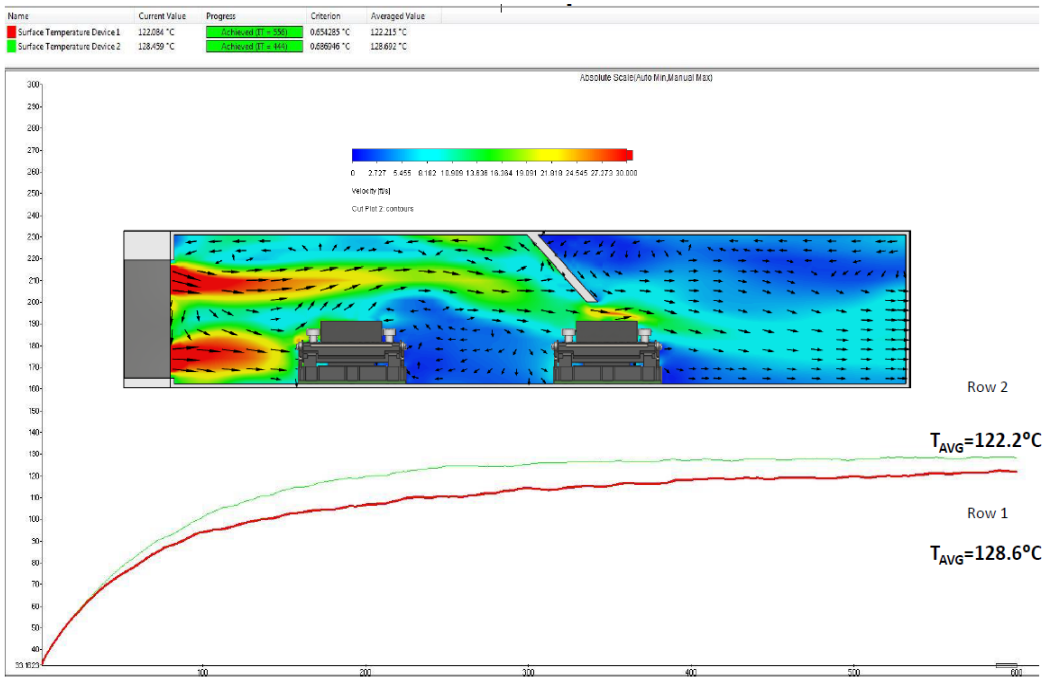

Figure 5-1 Results and Temperature Cut-plot with optimized position

Table 5-1 discusses the average case temperature difference between two sockets subjected to the various configuration as without defector, deflector at intuitive position and deflector at the optimized position.

Configuration	$T_{row\ 2} - T_{row1}$
Without deflector	81.3°C
Deflector at intuitive position	35°C
Deflector at optimized position	6.4°C

Table 5-1 Comparision with various configuration

By using optimized position the temperature uniformity between two sockets was achieved thus reducing the need to use efficient sockets for Row 2.

5.2 Future Work

Experimental validation can be done to an optimized model with the hypothesis and computational fluid dynamics used in this study. Once the experimental data is in good agreement with computational studies, optimization of air deflector orientation can be studied for different burn-in boards where the distance of socket differ from initial studies. Fabrication of Deflector can also be achieved in such a way that the input variables can be changed ergonomically for different burn-in boards.

References

[1] http://pdsius.com/what-is-burn-in/

[2] Thermal Testing of Burn-in Sockets- Forster et al. BiTS Workshop, Phoenix, AZ March 2-5,2003

[3] https://www.microcontrol.com/burn-in-boards/

[4] Sobachkin, A.; Dumnov, G. Numerical Basis of CAD-Embedded CFD. In Proceedings of the NAFEMS World Congress, Salzburg, Austria, 9 June 2013.

[5] Mani, D., Fernandes, J., Eiland, R., Agonafer, D., and Mulay, V., "Improving ducting to increase cooling performance of high-end web servers subjected to significant thermal shadowing – an experimental and computational study," 2015 31st Thermal Measurement, Modeling & Management Symposium (SEMI-THERM), San Jose, CA, 2015, pp. 319323.

[6] Pratik Bansode, Jimil Shah, Gautam Gupta, Dereje Agonafer, Harsh Patel, David Roe, Rick Tufty," Measurement of the Thermal Performance of a Single Phase Immersion Cooled Server at Elevated Temperatures for Prolonged Time Periods", ASME INTERPACK 2018-8432.

[7] G. Thirunavakkarasu, S. Saini, J.M. Shah, D. Agonafer, "Airflow Pattern and Path Flow Simulation of Airborne Particulate Contaminants in a High-Density Data Center Utilizing Airside Economization" Proceedings of the ASME 2018 International Technical Conference and Exhibition on Packaging and Integration of Electronic and Photonic Microsystems, Interpack 2018, San Francisco, CA, USA.

[8] Siddarth, Ashwin & Eiland, Rick & Fernandes, John & Agonafer, Dereje. (2018). Impact of Static Pressure Differential Between Supply Air and Return Exhaust on Server Level Performance. 953-961. 10.1109/ITHERM.2018.8419536

[9] Patil, S., Chintamani, S., Kumar, R., and Dennis, B. H., 2016. "Determination of orthotropic thermal conductivity in heat generating cylinder". ASME 2016 International Mechanical Engineering Congress and Exposition, American Society of Mechanical Engineer, pp-V011T15A016 doi:10.1115/IMECE2016-67918

[10] Patil, S., Chintamani, S., Grisham, J., Kumar, R., and Dennis, B., 2015. “Inverse Determination of Temperature Distribution in Partially Cooled Heat Generating Cylinder”. ASME 2015 International Mechanical Engineering Congress and Exposition , pp -V08BT10A024-V08BT10A024, doi:10.1115/IMECE2015-52124

[11] Fabela, Oscar, Patil, S., Chintamani, S., and Dennis, B., 2017. “Estimation of effective thermal conductivity of porous Media utilizing inverse heat transfer analysis on cylindrical configuration”. ASME 2017 International Mechanical Engineering Congress and Exposition,pp-V008T10A089-V008T10A089 doi:10.1115/IMECE2017-71559

[12] Upreti, R. , Patil,S. , Chintamani, S., Dennis,B., and Wang, B.P. ‘Stochastic Finite Element Thermal analysis of a ball grid array package’ , ASME Journal of Electronic Packaging

[13] Pavan Rajamane, Fahad Mirza, “Chip Package Interaction Study to Analyze the Mechanical Integrity of a 3-D TSV Package” - ASME Interpack 2015

[14] Kumar, Ashish & Shahi, Pardeep & K. Saha, Sandip. (2018). Experimental Study of Latent Heat Thermal Energy Storage System for Medium Temperature Solar Applications. 10.11159/htff18.152.

Biographical Information

Ajinkya received his Master of Science degree in Mechanical Engineering from The University of Texas at Arlington. He completed his bachelor's degree in Mechanical Engineering from North Maharashtra University, India. He had been working in the Electronic, MEMS and Nanoelectronics Systems Packaging Center labs at the University of Texas at Arlington and has an area of interest in heat transfer and optimization techniques. Ajinkya completed his internship in Plastronics Inc. and worked on design and optimization of various burn-in sockets for improving thermal performance.